# Temperature-dependent magnetization in diluted magnetic semiconductors

S. Das Sarma, E. H. Hwang, and A. Kaminski
*Condensed Matter Theory Center, Department of Physics, University of Maryland, College Park, Maryland 20742-4111*
(Received 24 November 2002; published 1 April 2003)

We calculate magnetization in magnetically doped semiconductors assuming a local exchange model of carrier-mediated ferromagnetic mechanism and using a number of complementary theoretical approaches. In general, we find that the results of our mean-field calculations, particularly the dynamical mean-field theory results, give excellent qualitative agreement with the experimentally observed magnetization in systems with itinerant charge carriers, such as $Ga_{1-x}Mn_xAs$ with $0.03<x<0.07$, whereas our percolation-theory-based calculations agree well with the existing data in strongly insulating materials, such as $Ge_{1-x}Mn_x$. We comment on the issue of non-mean-field like magnetization curves and on the observed incomplete saturation magnetization values in diluted magnetic semiconductors from our theoretical perspective. In agreement with experimental observations, we find the carrier density to be the crucial parameter determining the magnetization behavior. Our calculated dependence of magnetization on external magnetic field is also in excellent agreement with the existing experimental data.

DOI: 10.1103/PhysRevB.67.155201 PACS number(s): 75.50.Pp, 75.10.−b, 75.30.Hx

## I. INTRODUCTION

Diluted magnetic semiconductors (sometimes also referred to as doped magnetic semiconductors—we will use the abbreviation ''DMS'' to denote both of these equivalent terminologies) have recently attracted a great deal of attention[1,2] for their potential in combining ferromagnetic and semiconductor properties in a single material. The prototypical DMS material is $Ga_{1-x}Mn_xAs$ (Ref. 3) (typically $x\approx 1-10\%$) with the Mn ions substitutionally (in the ideal situation) replacing Ga at the cation sites. Mn ions in $Ga_{1-x}Mn_xAs$ serve a dual purpose, acting both as dopants (acceptors in this case) and as magnetic impurities, whose spins align at the ferromagnetic transition. For $x\approx 1-7\%$, $Ga_{1-x}Mn_xAs$ is found to be ferromagnetic with the ferromagnetic transition temperature (or, equivalently, the Curie temperature) $T_c\approx 10-100$ K. The optimum value of $x$, which corresponds to the highest value of reported value of $T_c$, is around 5%. Other DMS materials of current interest include $In_{1-x}Mn_xAs$,[4] $Ga_{1-x}Mn_xP$,[5] $Ge_{1-x}Mn_x$,[6] and $Ga_{1-x}Mn_xSb$.[7]

In spite of a great deal of recent experimental and theoretical activity,[1,2] there is not yet a consensus on the fundamental mechanism leading to ferromagnetism in these systems as well as on the definitive predictive theory quantitatively describing this ferromagnetic mechanism. It is, therefore, important to work out detailed and experimentally falsifiable consequences for various proposed theoretical models and ideas. In this context, it is unfortunate that much of the theoretical DMS literature, perhaps due to the considerable technological motivation in creating room-temperature ferromagnetic semiconductors for projected spintronics applications, has concentrated on the calculations of $T_c$ in various DMS materials. Such theoretical predictions of $T_c$ invariably involve tuning free parameters (e.g., the strength of the exchange coupling between carriers and local moments), whose values are often unknown *a priori*. This significantly reduces the practical importance of these predictions except perhaps in the broadest qualitative sense of identifying the crucial controlling parameters that determine and limit $T_c$ in DMS materials. On the other hand, the temperature dependence $M(T)$ of the spontaneous magnetization possesses many characteristics, such as concavity/convexity of the curve, value of saturation magnetization, critical behavior at the point of ferromagnetic transition, etc., which cannot all be described by just tuning parameters of a given model. Thus study of $M(T)$ has a very high potential for elucidating the physics behind DMS ferromagnetism in real systems.

A particular issue of considerable significance in DMS ferromagnetism has been the non-trivial non-mean-field-like behavior of the spontaneous magnetization as a function of temperature. This was already apparent in the very first reported observation[4] of DMS ferromagnetism in a $III_{1-x}Mn_xV$ material, namely, $In_{1-x}Mn_xAs$, where the experimental $M(T)$ curve exhibited an untypical outwardly concave shape strikingly different from the usual convex $M(T)$ behavior expected within the textbook Weiss mean-field theory[8] and seen routinely in conventional ferromagnetic materials. The $In_{1-x}Mn_xAs$ (with $x=0.013$) system studied in Ref. 4 was an insulating system (i.e., with resistivity increasing monotonically with decreasing temperature), and the insulating ferromagnetic DMS systems studied so far in the literature almost always exhibit qualitatively similar non-mean-field-like concave $M(T)$ behavior.[6]

Two of us have recently shown[9] that such a manifestly non-mean-field-like concave $M(T)$ behavior in insulating DMS materials can be understood on the basis of a magnetic percolation transition of bound magnetic polarons in the strongly localized carrier system. Earlier numerical simulations[10,11] in the strongly localized regime had already indicated that the $M(T)$ behavior of DMS ferromagnets could have concave outward shapes as seen experimentally. Very recent numerical simulations[12] in the strongly localized regime have verified our polaron percolation picture of DMS ferromagnetism in the insulating regime.

Even in the ''metallic'' (i.e., with resistivity decreasing with $T$ below the ferromagnetic transition temperature) DMS

 

systems,[1,3,13–20] such as optimally doped $Ga_{0.95}Mn_{0.05}As$, where long-range magnetic ordering of the Mn magnetic moments is created presumably by a dilute gas of delocalized holes mediating the magnetic interaction, the experimentally observed $M(T)$ often appears to be very different from the classic mean-field shape.[8] Although the metallic $Ga_{1-x}Mn_xAs$ DMS system does not exhibit the manifestly concave temperature-dependent magnetization seen in insulating DMS systems, the observed $M(T)$ in metallic DMS is often[1,3,13–20] almost linear in temperature for $0.5T_c \lesssim T < T_c$, with a temperature-dependent behavior intermediate between the concave $M(T)$ shapes of the localized theory[9] and the textbook convex magnetization curves.[8]

We mention that very recent annealing experiments[13–20] in $Ga_{1-x}Mn_xAs$ (with $x=0.05-0.10$) demonstrate that $M(T)$ behavior (as well as the value of $T_c$) can be strongly affected by annealing, and particularly, ''optimal'' annealing (to be found empirically for each sample purely by trial and error since the precise role of annealing in improving the materials quality is unknown at this stage) may lead to reasonably mean-field-like convex $M(T)$ shape with a concomitant enhancement of $T_c$. Nonoptimal annealing, on the other hand, leads to suppression of $T_c$ and strongly non-mean-field-like (and nonuniversal) $M(T)$ behavior.

Finally, most of DMS magnetization measurements in the literature, particularly for the insulating DMS systems, show a saturation magnetization (for $B=0$) considerably smaller in magnitude than that expected from the full ordering of all the magnetic ions, indicating that a large fraction (sometimes as much as 90%) of the magnetic ions do not contribute to the global DMS ferromagnetism.

Motivated by the desire for illuminating the physical mechanisms underlying DMS ferromagnetism, we theoretically consider in this paper the temperature-dependent magnetization $M(T)$ in three-dimensional DMS systems using a number of complementary theoretical approaches. The calculations we present here are based on the static (Weiss) molecular mean-field theory,[21] the dynamical mean-field theory (DMFT),[22] and the percolation theory.[23] Of particular interest is the important issue of correlations between magnetic and transport properties of various DMS materials since such correlations should (and do) exist in magnetic systems, where the ferromagnetism is mediated by carriers leading to the global ordering of the dopant local moments. While earlier studies invariably concentrated on either localized-carrier (''insulating'') and itinerant-carrier (metallic) material, we consider both these regimes as well as the crossover between them. We provide detailed numerical results for our calculated magnetization $M(T,B)$, where $B$ is the applied external magnetic field and $T$ is the temperature, in various regimes of the system parameter space. These $M(T,B)$ results should help ascertain the applicability of various theoretical models to specific experimental DMS materials of current interest.

This paper is organized as follows. In Sec. II, we describe our model and our theoretical approaches based on the Weiss mean-field theory, DMFT, and the percolation theory, and present our numerical results for $M(T,B)$ in each of the theoretical approaches, providing brief discussion of our results in light of the existing experimental data in the literature. We conclude in Sec. III, summarizing our qualitative findings and providing a critical perspective on what our theoretical results on magnetization imply for the microscopic mechanisms underlying DMS ferromagnetism with the particular emphasis on the correlations between transport characteristics (metallic or insulating) and $M(T)$ behavior (convex, concave, or ''linear'').

## II. MODEL, THEORY, AND RESULTS

### A. The model

We assume in this work that the fundamental mechanism underlying ferromagnetism in DMS materials (e.g., $III_{1-x}Mn_xV$, $Ge_{1-x}Mn_x$) is the carrier—local-moment (kinetic or $p$-$d$) exchange coupling, which eventually leads to a global ferromagnetic ordering of the impurity local moments (i.e., Mn) for $T<T_c$ overcoming any direct antiferromagnetic (superexchange) interaction between the local moment spins themselves. This is certainly the prevalent viewpoint for DMS ferromagnetism, at least for $Ga_{1-x}Mn_xAs$ system following the pioneering work of Ohno and his co-workers. It is natural to ask about the evidence for this belief in carrier-mediated DMS ferromagnetism induced in the Mn local moments. First-principles band theory calculations indicate that there is strong $p$-$d$ hybridization between the Mn $d$ levels and the valence-band $p$ states of GaAs. This leads to strong kinetic exchange coupling between hole spins and Mn spins, which is the basis of our model. Experimentally, there are a number of compelling circumstantial indications of $Ga_{1-x}Mn_xAs$ being a carrier-mediated ferromagnetic material. First, there is a strong correlation (made even stronger by the recent annealing experiments) between transport and magnetic properties. This, however, is not definitively conclusive since strongly insulating $Ga_{1-x}Mn_xAs$ (and $In_{1-x}Mn_xAs$) samples are also found to be ferromagnetic (albeit with much lower $T_c$ values). Perhaps the most compelling evidence supporting the carrier-mediated ferromagnetic mechanism, is the observed agreement (so far available only in $Ga_{1-x}Mn_xAs$ DMS systems) between the magnetization measured directly using a SQUID magnetometer and that inferred by analyzing the anomalous Hall-effect data. Such an consistency between direct and ''transport-inferred'' magnetization strongly suggests a carrier-mediated exchange mechanism underlying DMS ferromagnetism. In addition, there are a number of experiments dealing with optical properties (again, available only for $Ga_{1-x}Mn_xAs$ so far) which indicate very strong correlation between the magnetic band structure and the magnetization of the system, leading again to the condition that the global ferromagnetic ordering of the Mn local moments is most likely induced by the hole spin polarization in DMS systems. The related issue of whether these carriers are valence-band holes or impurity band holes is more difficult to settle. Given the strong inherent disorder in DMS materials and rather strong exchange coupling between hole and Mn spins (leading to local binding of holes and Mn ions), it is natural to think that all of the physics (both localized and delocalized) are essentially impurity band physics. This viewpoint, which we have adopted in our theories presented in this paper, has received strong support from recent optical experiments. Also our DMFT results, as presented in Sec. II C, clearly demonstrate the important role of impurity band physics in DMS magnetic properties.

Since the most intensively studied DMS materials of current interest are Mn-doped III-V semiconductors $III_{1-x}Mn_xV$ (e. g., $Ga_{1-x}Mn_xAs$, $In_{1-x}Mn_xAs$, $Ga_{1-x}Mn_xP$, $Ga_{1-x}Mn_xN$, and $Ga_{1-x}Mn_xSb$), where the carriers are typically holes, we will other refer to the semiconductor carriers as ''holes'' in the rest of the paper without any loss of generality.

So our basic model is that of a finite density $n_i$ of magnetic dopants (''impurities'') interacting through a local exchange coupling with a finite density $n_c$ of holes in the host semiconductor material with $n_c/n_i \ll 1$. We assume that magnetic impurities under consideration enter substitutionally at the cation sites (e.g., Mn impurities at Ga sites). Recent experimental annealing studies of $Ga_{1-x}Mn_xAs$ have shown[13–19] that lattice defects may be playing an important role in determining magnetic and transport properties of the samples, but we assume in our work that these defects enter our theory only in determining the basic parameters of the model, namely, the density of magnetically active dopants $n_i$, the hole density $n_c$, and perhaps the local effective exchange coupling $J$ between the holes and the magnetic impurities, and do not include any defects into our model explicitly. Examples of such defects, which enter our model through its parameters rather than directly, are given by antisite defects in the host semiconductor material (i.e., As at Ga sites in GaAs) and Mn interstitials (i.e., Mn atoms at interstitial sites rather than cation substitutional sites), which may very well be important in providing substantial compensation in the semiconductor, leading to the experimental fact that the hole density $n_c$ is usually a small fraction of the magnetic dopant density instead of there being a one-to-one correspondence between dopants and holes. The local-moment density $n_i$ in our model is not necessarily the total Mn concentration in the system, since the presence of Mn interstitial defects could lower the density of magnetically active Mn ions. In this work, we use $n_i$ to denote local-moment volume density and $x$ to denote the fraction of Ga atoms replaced by Mn dopants.

Similarly, consistent with the spirit of our minimal model we also neglect all band structure effects in our theory, making the simplest approximation such as a single parabolic band with a single effective mass or a single simple tight-binding carrier band characterized by an effective band width parameter. This is not because realistic band-structure effects are not of any importance in DMS ferromagnetism, in fact we believe that spin-orbit coupling in $Ga_{1-x}Mn_xAs$ valence-band hole states may play a quantitative role in $Ga_{1-x}Mn_xAs$ ferromagnetism, particularly in the relatively disorder-free metallic ($x \approx 0.05$) systems where the holes are likely to be GaAs valence-band hole states with strong spin-orbit coupling. Our reasons for neglecting spin-orbit coupling and other band-structure effects in our theory are the following: (1) our interest in this paper is in theoretically exploring $M(T,B)$ within a minimal model, which requires only $n_i$, $n_c$, and $J$, leaving out all nonessential complications; (2) if needed, band-structure effects can be systematically included in the future by appropriately extending the model; (3) due to the inevitable presence of strong exchange coupling and strong disorder in DMS materials, a starting point based on perfect ''realistic'' valence-band hole states may be inapplicable—in fact, we believe that much of the DMS physics is occurring in the impurity band of the host semiconductor with the itinerant and the localized carriers being the extended and the localized hole states in the impurity band of the system and not the valence-band states, a view point strongly supported by several recent experimental results.[24–27]

The Hamiltonian of exchange interaction between magnetic impurities and holes, we use in this paper, reads

$$H_M = \int d^3r \sum_j J a_0^3 [\mathbf{S}_j \cdot \mathbf{s}(\mathbf{r})] \delta(\mathbf{r}-\mathbf{R}_j) \equiv \sum_j J a_0^3 [\mathbf{S}_j \cdot \mathbf{s}(\mathbf{R}_j)], \tag{1}$$

where $J$, which has units of energy, is the exchange coupling between an impurity spins $\mathbf{S}_j$ located at $\mathbf{R}_j$ and a hole spin density $\mathbf{s}(\mathbf{r})$, and $a_0^3$ is the unit cell volume needed for proper normalization. The impurity spin $\mathbf{S}$ in Eq. (1) is assumed to be completely classical in the theory whereas the carrier spin $\mathbf{s}$ is treated quantum mechanically. This is justified because the impurity spin is large, e.g., $S=5/2$ for Mn in $Ga_{1-x}Mn_xAs$.

Our model (except for the mean-field theory considerations of Sec. II B) omits the direct Mn-Mn antiferromagnetic exchange interaction, assuming its effects to be either negligibly small or incorporated into the effective parameters of the model. Actually, in the parameter range of interest to us ($x \ll 1$), where DMS ferromagnetism typically occurs, the magnetic impurities are separated from each other by non magnetic atoms, and this antiferromagnetic interaction, which rapidly decays with the distance, should be negligible. We also ignore any specific hole-hole interaction effect in our theory. These approximations are nonessential and are done in the spirit of identifying the minimal DMS magnetic model of interest. Both of these effects, which may be of quantitative importance in some situations, can be included in the theory by adjusting the parameters of the model, or perhaps at the cost of introducing more unknown parameters characterizing these interactions. The possible effects of including these interactions in our calculations will be discussed later in the paper.

With this introduction, the full Hamiltonian is given by

$$\begin{aligned} H = & \int d^3r \sum_\alpha \psi_\alpha^\dagger(\mathbf{r}) \left[ -\frac{\nabla^2}{2m} + V(\mathbf{r}) \right] \psi_\alpha(\mathbf{r}) \\ & + \sum_j \int d^3r \left[ \sum_\alpha W(\mathbf{r}-\mathbf{R}_j) \psi_\alpha^\dagger(\mathbf{r}) \psi_\alpha(\mathbf{r}) \right. \\ & \left. + \sum_{\alpha\beta} J a_0^3 (\mathbf{S}_j \cdot \boldsymbol{\sigma}_{\alpha\beta}) \delta(\mathbf{r}-\mathbf{R}_j) \psi_\alpha^\dagger(\mathbf{r}) \psi_\beta(\mathbf{r}) \right] \\ & + \sum_j g_i \mu_B (\mathbf{S}_j \cdot \mathbf{B}) \\ & + \int d^3r \sum_{\alpha\beta} g_c \mu_B \psi_\alpha^\dagger(\mathbf{r}) \psi_\beta(\mathbf{r}) (\boldsymbol{\sigma}_{\alpha\beta} \cdot \mathbf{B}), \end{aligned} \tag{2}$$

where first term is the ''band'' Hamiltonian, with $m$ being the relevant effective mass, $V(\mathbf{r})$ is the random potential arising

from (nonmagnetic) disorder, $W(\mathbf{r}-\mathbf{R}_i)$ is the Coulomb potential due to a magnetic impurity located at $\mathbf{R}_i$, and the second term is the local exchange coupling between the moments of magnetic impurities and the carrier spins [i.e., precisely the $H_M$ defined by Eq. (1)]. For the Pauli matrices, we use the notation $\boldsymbol{\sigma}_{\alpha\beta}\equiv(\sigma^x_{\alpha\beta},\sigma^y_{\alpha\beta},\sigma^z_{\alpha\beta})$ with $\alpha$ and $\beta$ being the spin indices and $(\boldsymbol{\sigma}_{\alpha\beta}\cdot\mathbf{a})\equiv a_x\sigma^x_{\alpha\beta}+a_y\sigma^y_{\alpha\beta}+a_z\sigma^z_{\alpha\beta}$ for any vector **a**. The last two terms in Eq. (2) are simply the Zeeman energies of the local moments and the holes, respectively, $g_{\mathrm{i}}$ and $g_{\mathrm{c}}$ are the corresponding $g$ factors, $\mu_B$ is the Bohr magneton, and **B** is the external magnetic field.

The local exchange coupling can be ferromagnetic ($J<0$) or antiferromagnetic ($J>0$), without affecting DMS ferromagnetism [first-principles band theory[28–30] suggests local antiferromagnetic coupling ($J>0$) for the holes in $Ga_{1-x}Mn_xAs$]. Finally, we mention that the magnetic interaction Hamiltonian, defined by Eq. (1), is sometimes referred to as the $s$-$d$ (or $s$-$f$) exchange Hamiltonian[31] or the Zener model[32] in the literature although it was originally introduced[33] by Nabarro and Fröhlich in a slightly different context. The physics, we are interested in, is how the local exchange interaction defined in Eqs. (1) and (2) could lead to global ferromagnetic ordering of the impurity local moments below a Curie temperature $T_c$. We mention that we choose $S=5/2$ and $s=1/2$ in all our numerical calculations below.

Unfortunately, none of the parameters $J$, $n_{\mathrm{c}}$, and $n_{\mathrm{i}}$ of our model is directly experimentally measurable. This is why we have emphasized, throughout this work, qualitative behavior in temperature-dependent magnetization as a function of the system parameters. The carrier density $n_{\mathrm{c}}$ is hard to measure even in metallic ferromagnetic materials because of the problems associated with anomalous Hall effect (and the situation is obviously worse in strongly insulting systems). The local-moment density $n_{\mathrm{i}}$ is unknown because only a fraction of the incorporated Mn atoms are magnetically active due to the invariable presence of Mn interstitials and other possible defects in the system. What is known about $Ga_{1-x}Mn_xAs$ is that it is a heavily compensated system in the sense that the density of holes, is much less than the density of Mn, typically $n_{\mathrm{c}}/n_{\mathrm{i}}\sim 0.1$. Much of this compensation most likely arises from various defects invariably present in low-temperature molecular beam epitaxy grown $Ga_{1-x}Mn_xAs$. The two most ''harmful'' defects in this respect are Mn interstitials and As antisites. Both of these defects act as effective double donors, producing two electrons each. Thus the holes produced by the magnetically and electrically active ''desirable'' $Mn^{2+}$ ions (sitting at substitutional cation sites), with each substitutional Mn ion producing one hole, could be heavily compensated by the defects leading to the existing situation in $Ga_{1-x}Mn_xAs$, where $n_{\mathrm{c}}/n_{\mathrm{i}}\ll 1$.

All aspects of Kondo physics are completely negligible for the current problem. Kondo physics is relevant only in the complementary regime of high carrier density ($n_{\mathrm{c}}/n_{\mathrm{i}}\gg 1$), where a paramagnetic carrier ground state entails as the impurity spin is quenched by the free carriers. For itinerant delocalized carriers (i.e., metallic DMS), the indirect exchange coupling between the local moments (induced by carrier spin polarization) is precisely the Rudermann-Kittel-Kasuya-Yosida (RKKY) interaction. The relevance (or perhaps even, the dominance) of RKKY physics (leading to a magnetic ground state) over the Kondo physics in the low carrier density limit of the Kondo lattice system has occasionally been mentioned in the Kondo-effect literature.[34]

The crucial element of RKKY physics, playing a key role in DMS ferromagnetism, is the relatively low values of carrier density in these materials leading to $k_F\sqrt[3]{n_{\mathrm{i}}}\ll 1$ (where $k_F$ is the Fermi wavevector associated with the carrier density $n_{\mathrm{c}}$ and $\sqrt[3]{n_{\mathrm{i}}}$ is the characteristic interimpurity separation) so that the RKKY interaction is essentially always ferromagnetic, and the RKKY spin-glass-type behavior predominant in disordered magnetic metallic systems may not arise here since the interaction is mostly ferromagnetic avoiding effects of frustration.

In principle, one could start from the general Hamiltonian (2), and try to develop a theory for carrier localization and magnetism on an equal footing. Such an ambitious attempt would be essentially futile, due to the enormous complexity of the problem, which would require both disorder and exchange interaction to be treated nonperturbatively. We, therefore, adopt the reasonable empirical approach of building into our basic model the metallic (itinerant carriers) or the insulating (localized carriers) nature of the system, and develop separate complementary theoretical approaches for the two situations in order to compare and contrast the nature of DMS ferromagnetism in metallic and insulating systems, both with the local exchange magnetic Hamiltonian (1) coupling the impurity moments to carrier spins.

We use complementary theoretical approaches [degenerate- and nondegenerate-carrier Weiss static mean-field theory, dynamical mean-field theory, and percolation theory] in this paper; two of which apply to the limiting cases of extended metallic system (degenerate-carrier mean-field theory and DMFT) and the other two to the strongly localized insulating system (nondegenerate-carrier mean-field theory and percolation theory). In principle, DMFT can interpolate smoothly between the systems with extended and localized carriers, but we have neglected localization effects in our DMFT calculations carried out so far. Our results for temperature- and magnetic-field-dependent magnetization $M(T,B)$ exhibit qualitative behavior very similar to that seen in experiments which, given the minimal nature of our theoretical model, is all we can expect of the theory. In our view, at this early stage of the development of DMS materials and their physical understanding (and given the metastable and fragile complex nature of the DMS systems), where all the materials details (e.g., defects and disorder of many possible types) qualitatively affecting the system magnetization may not even be known at the present time, it is premature to demand (or impose, for example, by tuning the parameters of the theoretical model) quantitative agreement between theory and experiment. In this respect, we strongly disagree with the statements asserting that DMS ferromagnetism is a well-understood problem based on a model of free valence-band holes interacting with Mn local moments. The excellent qualitative agreement between our calculated magnetization results in different theoretical approaches and the experimental magnetization data in the existing literature

provides useful insight into the possible magnetic mechanisms underlying metallic and insulating DMS systems.

### B. The Static Mean-Field Theory

The basic idea underlying the static mean-field theory, as applied to ferromagnetism in DMS, is to represent action of all impurity/hole spins upon a given impurity/hole spin as an effective ''mean field,'' whose value is determined by the average values of the spins acting upon this given spin. The resulting equations for the spins of impurities and holes are to be solved self-consistently, finally, yielding the equilibrium magnetization at a given temperature.

The difference between the mean-field theory, considered in this section, and the canonical Weiss mean-field model arises from the existence of two interacting species of spins, those of holes and of impurities in a DMS system. As a result, we have two effective fields—one determined by the average value of a hole spin and the other determined by the average value of an impurity spin. In the framework of Hamiltonian (2), the effective field acting upon holes has contributions coming from magnetic impurities and from the external magnetic field **B**,

$$B_{\rm eff}^{(\rm c)}=\frac{1}{g_{\rm c}\mu_B}(Ja_0^3 n_{\rm i}\langle S_z\rangle)+B, \tag{3}$$

where the direction of the $z$ axis is chosen to coincide with the direction of applied magnetic field **B**, or, in the case of $B=0$, with the direction of spontaneous magnetization of impurities. The effective field acting upon impurities is a sum of contributions from holes and the external magnetic field. Relative simplicity of the static mean-field theory allows us to account also for possible direct antiferromagnetic interaction between magnetic impurities by adding the following term to the Hamiltonian:

$$H_{\rm AF}=\sum_{jk} J_{jk}^{\rm AF}(\mathbf{S}_j\cdot\mathbf{S}_k), \tag{4}$$

which yields one more contribution to the effective field acting upon magnetic impurities,

$$B_{\rm eff}^{(\rm i)}=\frac{1}{g_{\rm i}\mu_B}(z^{\rm AF}J^{\rm AF}\langle S_z\rangle+Ja_0^3 n_{\rm c}\langle s_z\rangle)+B, \tag{5}$$

where $z^{\rm AF}$ is the effective number of surrounding impurities a given impurity interacts with.

The response of the impurity spin to this effective field $B_{\rm eff}^{(\rm i)}$ is given by

$$\langle S_z\rangle=S\mathcal{B}_S\left(\frac{g_{\rm i}\mu_B B_{\rm eff}^{(\rm i)}}{k_BT}\right), \tag{6}$$

where

$$\mathcal{B}_s(x)\equiv\frac{2s+1}{2s}\coth\frac{2s+1}{2s}x-\frac{1}{2s}\coth\frac{1}{2s}x \tag{7}$$

is the Brillouin function. The magnetic response of hole spins to effective field $B_{\rm eff}^{(\rm c)}$ produced by impurities strongly depends on whether the hole gas is degenerate or not. The two complementary cases of nondegenerate and degenerate holes will be considered below in Secs. II B 1 and II B 2, respectively. We mention that the nondegenerate (degenerate) situation applies primarily to the insulating (metallic) DMS systems.

#### 1. Nondegenerate holes

The case of nondegenerate holes, when the hole spin distribution is not affected by the Pauli exclusion principle, corresponds to two physical situations. The first one occurs when the holes are localized with strong on-site repulsion, so there is only one hole at each localization center. This scenario is relevant to DMS with localized carriers, which will also be considered in Sec. II D using the percolation theory. The second situation takes place in a gas of delocalized holes when the temperature is higher than the Fermi energy.

When the Pauli exclusion principle plays no role in the spin distribution of electrons, the latter is determined by Boltzmann statistics, and the average hole spin, as determined by the effective mean-field $B_{\rm eff}^{(\rm c)}$, is given by

$$\langle s_z\rangle=s\mathcal{B}_s\left(\frac{g_{\rm c}\mu_B B_{\rm eff}^{(\rm c)}}{k_BT}\right), \tag{8}$$

similarly to Eq. (6), with $g_{\rm c}$ being the hole $g$ factor.

Combining Eqs. (3), (5), (6), and (8), we obtain the following self-consistent equation for $\langle S_z\rangle$:

$$\begin{aligned}\frac{\langle S_z\rangle}{S}=\mathcal{B}_S\Bigg[&-3\frac{T_{c0}}{T}\sqrt{\frac{n_{\rm c}}{n_{\rm i}}}\sqrt{\frac{sS}{(s+1)(S+1)}}\\&\times\mathcal{B}_s\Bigg(-3\frac{T_{c0}}{T}\sqrt{\frac{n_{\rm i}}{n_{\rm c}}}\sqrt{\frac{sS}{(s+1)(S+1)}}\frac{\langle S_z\rangle}{S}\\&+\frac{g_{\rm c}\mu_B B}{k_BT}\Bigg)+\frac{6ST_1}{(S+1)T}\frac{\langle S_z\rangle}{S}-\frac{g_{\rm i}\mu_B B}{k_BT}\Bigg],\end{aligned} \tag{9}$$

where

$$k_BT_{c0}=\tfrac{1}{3}Ja_0^3\sqrt{n_{\rm c}n_{\rm i}}\sqrt{S(S+1)s(s+1)}, \tag{10}$$

$$k_BT_1=\tfrac{1}{6}S(S+1)z^{\rm AF}J^{\rm AF}, \tag{11}$$

and $J$ is assumed to be negative (antiferromagnetic interaction between impurities and holes). Similarly to the textbook mean-field theory, Eq. (9) has a nontrivial solution in the absence of the external magnetic field only if temperature $T$ is below a certain value, which is the ferromagnetic transition temperature $T_c$. Using the expansion for the Brillouin function

$$\mathcal{B}_s(x)\big|_{x\ll 1}\approx\frac{s+1}{3s}x+O(x^3), \tag{12}$$

we arrive at the following expression:

$$T_c^{(\rm n)}=\sqrt{T_{c0}^2+T_1^2}-T_1. \tag{13}$$

In the absence of antiferromagnetic interaction between the impurities, $T_1=0$ so the ferromagnetic transition tem-

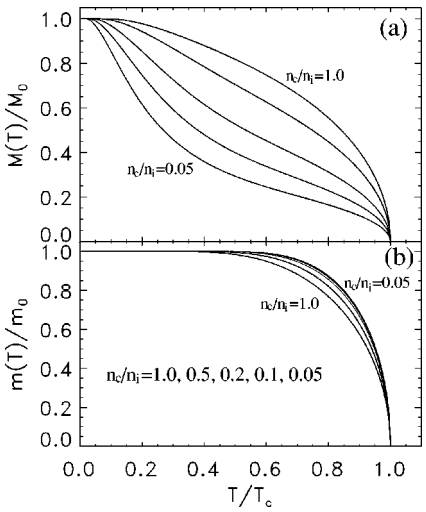


FIG. 1. (a) Dopant magnetization $M/M_0 \equiv \langle S_z \rangle / S$ and (b) hole magnetization $m/m_0 \equiv \langle s_z \rangle / s$ with $S=5/2$ and $s=1/2$ from the nondegenerate-hole model for various values of density ratio $(n_c/n_i = 1.0, 0.5, 0.2, 0.1, 0.05)$.

perature equals $T_{c0}$. Equation (9) in the absence of the external magnetic field and at $J^{AF}=0$ reduces to

$$\frac{\langle S_z \rangle}{S} = \mathcal{B}_S\left[ 3\frac{T_{c0}}{T}\sqrt{\frac{n_c}{n_i}}\sqrt{\frac{sS}{(s+1)(S+1)}} \times \mathcal{B}_s\left( 3\frac{T_{c0}}{T}\sqrt{\frac{n_i}{n_c}}\sqrt{\frac{sS}{(s+1)(S+1)}}\frac{\langle S_z \rangle}{S}\right)\right], \quad (14)$$

the average hole spin is still given by Eqs. (8) and (3) with $B=0$. The solution of Eq. (14) can be found numerically. The resulting magnetization curves for impurities and holes for several values of $n_c/n_i$ are shown in Fig. 1. Note that specific values of $J$, $n_i$, and $n_c$ are not of any relevance here—only the ratio $n_c/n_i$ is the important tuning parameter in determining magnetization as a function of $T/T_c$. The most important salient feature of Fig. 1 is the highly "non-mean-field-like" concave magnetization behavior for low values ($\leqslant 0.2$) of $n_c/n_i$. The reason for such behavior is that if we have one hole per many impurities, the effective field $B_{\rm eff}^{(c)}$ acting on holes is much stronger than its counterpart $B_{\rm eff}^{(i)}$ acting on impurities. As a result, the hole magnetization grows as

$$\frac{\langle s_z \rangle}{s} \sim \sqrt{\frac{T_{c0}^{(n)} - T}{T}}$$

for $T \lesssim T_{c0}$ and reaches unity at some temperature of the order of $T_{c0}$, while the impurity magnetization is still much less than unity. As the temperature is getting lower, the impurity magnetization grows as

$$\frac{\langle S_z \rangle}{S} \approx \mathcal{B}_S\left( 3\frac{T_{c0}^{(n)}}{T}\sqrt{\frac{n_c}{n_i}}\sqrt{\frac{sS}{(s+1)(S+1)}}\right)$$

and approaches unity only at

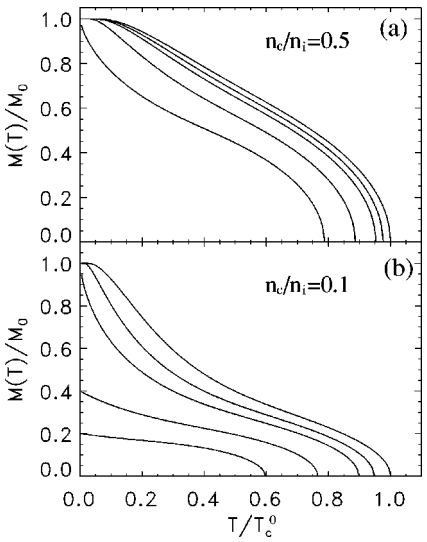


FIG. 2. Dopant magnetization with both $J^{AF}$ and $J$ from the nondegenerate-hole model with $S=5/2$ and $s=1/2$ for various values of coupling constant ratio ($z^{AF}J^{AF}/J = 0.0, 0.5, 1.0, 2.5$, and $5.0 \times 10^{-3}$, from the top) (a) for density ratios $n_c/n_i = 0.5$ and (b) $n_c/n_i = 0.1$.

$$T \sim T_{c0}^{(n)}\sqrt{\frac{n_c}{n_i}} \ll T_{c0}^{(n)}.$$

Finite antiferromagnetic coupling $J^{AF}$ suppresses $T_c$, as one can easily see from Eq. (13). In Fig. 2, we show the dopant magnetization, as given by the (numerical) solution of Eq. (9) for $B=0$, for various values of $T_1/T_{c0}$ for two typical values of $n_c/n_i = 0.5$ and 0.1.

In discussing the results shown in Fig. 2, we first note that the actual direct Mn-Mn antiferromagnetic coupling $J^{AF}$ is expected to be very small in $Ga_{1-x}Mn_xAs$ for low values of $x$, i.e., for relatively large Mn-Mn separation, since the direct antiferromagnetic coupling falls off exponentially with interatomic distance. For larger values of $x$, however, effects of antiferromagnetic Mn-Mn coupling may very well be important in determining the DMS magnetic behavior. In general, finite $J^{AF}$ suppresses both $T_c$ and $M(T)$ as one would expect. In particular, the zero-temperature magnetization $M(T \to 0)$ could be strongly suppressed far below the saturation magnetization by the finite antiferromagnetic coupling, particularly for lower hole densities,

$$\frac{\langle S_z \rangle}{S}\Big|_{T\to 0} = \min\left\{ 1, \frac{1}{2}\frac{T_{c0}^{(n)}}{T_1}\sqrt{\frac{n_c}{n_i}}\sqrt{\frac{S+1}{S}\frac{s}{s+1}}\right\}. \quad (15)$$

An interesting feature of Fig. 2 is that at low carrier densities, larger values of $J^{AF}$ may actually restore (albeit with strongly suppressed value of saturation magnetization) the convex $M(T)$ shape [e.g., the $z^{AF}|J^{AF}|/J = 5.0 \times 10^{-3}$ curve for $n_c/n_i = 0.1$ in Fig. 2(b)]. For higher hole densities, however, $M(T)$ becomes more concave for $J^{AF} \neq 0$.

The magnetic susceptibility of the system is essentially that of impurities (since $n_c/n_i \ll 1$ and $S > s$), and above the critical temperature is given by

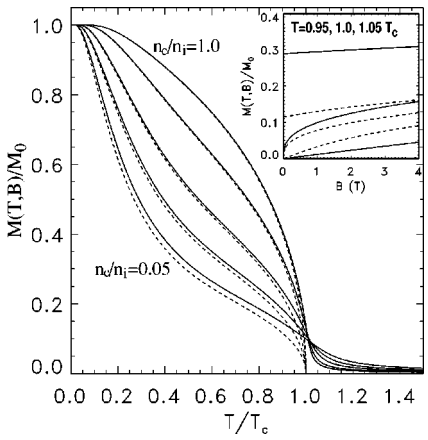


FIG. 3. External magnetic field and temperature dependence of dopant magnetization for the nondegenerate-hole model for various values of density ratio ($n_c/n_i=1.0,0.5,0.2,0.1,0.05$, from the top). Solid (dashed) lines indicate the results for a fixed external magnetic field $B=2.6T$ ($0T$). The parameters of Fig. 1 are used. In the inset, the magnetization curves as a function of magnetic field are given for fixed temperatures ($T=0.95$, 1.0, and $1.05T_c$, from the top). Solid (dashed) lines represent the results for $n_c/n_i=1.0$ ($n_c/n_i=0.1$).

$$\chi(T)\equiv n_i\frac{\partial(g_i\mu_B\langle S_z\rangle)}{\partial B}=\frac{\chi_0+\dfrac{(T_{c0}^{(n)})^2}{T^2Ja_0^3}g_ig_c\mu_B^2}{\left(1-\dfrac{T_c^{(n)}}{T}\right)\left(1+\dfrac{T^*}{T}\right)}, \quad (16)$$

where $T^*\equiv T_1+\sqrt{T_1^2+T_{c0}^2}$, and $\chi_0=n_i(g_i\mu_B)^2S(S+1)/3T$ is the paramagnetic susceptibility of bare impurities.

Finally, we show in Fig. 3 the effect of an external magnetic field, by showing $M(T,B)$ for fixed parameter values $J,S,s$, and for various values of density ratio $n_c/n_i$. In the main figure we show $M(T,B)$ as a function of temperature for a magnetic field value, $B=2.6T$ (solid lines), and in the inset we show $M(T,B)$ as a function of the external magnetic field for different temperatures. In inset we show $M(B,T_c)\propto B^{1/3}$, as expected in the mean-field theory.

#### *2. Degenerate hole gas*

For metallic DMS systems, where ferromagnetic $T_c$ is optimum (at least for $Ga_{1-x}Mn_xAs$), the carrier system is typically delocalized, with the Fermi energy substantially exceeding the ferromagnetic transition temperature. In such systems, the formalism of Sec. II B 1, developed for the nondegenerate-hole system is not applicable anymore, and we have to use the generic expression

$$\frac{\langle s_z\rangle}{s}=\frac{1}{n_c}\frac{1}{2}\int d\varepsilon f(\epsilon)[D(\varepsilon+g_c\mu_BsB_{\rm eff}^{(c)}) - D(\varepsilon-g_c\mu_BsB_{\rm eff}^{(c)})] \quad (17)$$

for the hole polarization, where $D(\varepsilon)$ is the hole density of states.

If the effective field $B_{\rm eff}^{(c)}$ acting on carriers is weak, we can expand the density of states up to the first order in the effective field to obtain

$$\frac{\langle s_z\rangle}{s}=\frac{1}{n_c}g_c\mu_BsB_{\rm eff}^{(c)}\int d\varepsilon f(\epsilon)D'(\varepsilon). \quad (18)$$

For very low temperatures, $k_BT\ll E_F$ (in general, this condition is satisfied in metallic $Ga_{1-x}Mn_xAs$ systems, where typically $k_BT_c/E_F<0.1$ noting that both $T_c$ and $E_F$ decrease with lowering the hole density $n_c$), we get

$$\frac{\langle s_z\rangle}{s}=\frac{1}{n_c}g_c\mu_BsB_{\rm eff}^{(c)}D'(E_F). \quad (19)$$

Linearizing Eq. (6) and using Eqs. (3) and (5), we arrive at

$$T_c^{(d)}=T_{c0}^{(d)}-2T_1, \quad (20)$$

where

$$T_{c0}^{(d)}=\frac{S(S+1)}{3}s^2(Ja_0^3)^2D(E_F)n_i \quad (21)$$

and $T_1$ is given by Eq. (11).

In the absence of antiferromagnetic interaction between magnetic impurities, $J^{AF}=0$, the ferromagnetic transition temperature equals $T_{c0}$. As one can see from Eq. (21), $T_{c0}\propto J^2n_c^{1/3}$ in the Weiss mean-field theory for degenerate holes [since $D(E_F)\propto n_c^{1/3}$ for a three-dimensional degenerate electron gas], in contrast to the nondegenerate case considered in Sec. II B 1, where $T_{c0}\propto Jn_c^{1/2}$.

When the hole density is very small, the hole Fermi energy $E_F$ may be comparable to the effective magnetic energy $g_c\mu_BsB_{\rm eff}^{(c)}$. In this case, we can not expand Eq. (17) with respect to the effective field $B_{\rm eff}^{(c)}$, and the hole magnetization must be obtained by directly integrating Eq. (17).

Before presenting our numerical results for the calculated temperature-dependent DMS magnetization for the degenerate-carrier mean-field theory, we mention that Eq. (20) for the ferromagnetic transition temperature in the Zener model was first derived in Ref. 35 more than 40 years ago and has recently been rediscovered[36,37] in the context of DMS ferromagnetism.

In Fig. 4, we show our calculated impurity and carrier magnetization for the degenerate-carrier Weiss mean-field theory using the same parameters (typical for $Ga_{1-x}Mn_xAs$) as for the corresponding nondegenerate case shown in Fig. 1. In general, except for the lowest hole density with $n_i/n_c=0.05$, the impurity magnetization is convex, but looks quite different from the classic textbook Weiss form except perhaps at very high carrier densities when $n_i/n_c\approx 1$. Particularly, for the realistic value of $n_c/n_i=0.1$ (which is thought to apply to many $Ga_{1-x}Mn_xAs$ samples), $M(T)$ in Fig. 4 has the non-mean-field-like straight line shape at lower temperatures. For higher values of hole density, $n_c/n_i=0.2$ and 0.5, the magnetization is much closer to the classical Brillouin shape whereas for lower carrier densities (e.g., $n_c/n_i$

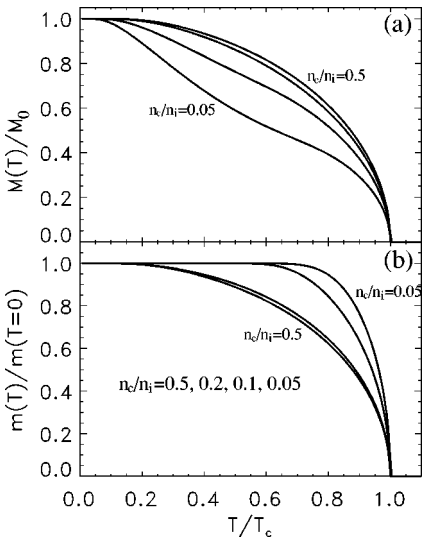


FIG. 4. (a) Dopant magnetizations from the degenerate-hole model for various values of the density ratio ($n_c/n_i=0.5$, 0.2, 0.1, and 0.05, from the top). Here we use the fixed parameter values: $S=5/2$, $s=1/2$, $n_i=10^{21}$ cm$^{-3}$, $m=0.5m_e$, $x=0.05$, and coupling constant $J=3.0$ eV. (b) Hole magnetization with the same parameters as in (a). Note $m(T=0)$ is the magnetization at $T=0$, which may not be equal to $m_0 \equiv g_c \mu_B s n_c$.

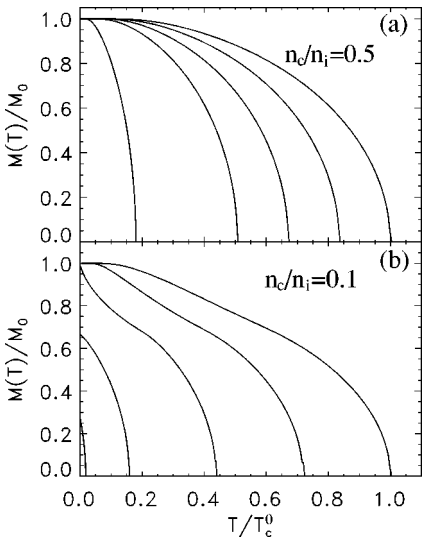


FIG. 5. Dopant magnetization with both $J^{AF} \neq 0$ from the degenerate-hole model for various values of the coupling constant ratio (a) $z^{AF}J^{AF}/J=0.0$, 0.5, 1.0, 1.5, and $2.5\times10^{-3}$ (from the top) and for density ratio $n_c/n_i=0.5$; (b) $z^{AF}J^{AF}/J=0.0$, 0.5, 1.0, 1.5, and $1.75\times10^{-3}$ (from the top) and $n_c/n_i=0.1$. The parameter values of Fig. 4 are used.

$=0.05$), even this metallic DMS system starts exhibiting the concave magnetization curve typical of the insulating DMS systems discussed Sec. II B 1.

The origin of the concave shape of the magnetization curve is exactly the same as for the nondegenerate case discussed in Sec. II B 1, namely, the magnetization of holes saturates at $T \lesssim T_{c0}$, much earlier than magnetization of impurities, which upon saturation of the hole magnetization grows as given by Eq. (14), which represents a concave curve provided $n_c/n_i \ll 1$. Thus, the concave magnetization behavior may be generic to the low carrier density limit of the DMS ferromagnets, independent of whether they are metallic or insulating although the highly concave magnetization curves of Fig. 1(a) are clearly much more typical of the insulating DMS systems than the metallic ones. The carrier magnetization results presented in Fig. 4(b) are very similar to textbook convex Weiss magnetization behavior. We note that the degenerate-carrier mean-field theory results shown in Fig. 4(a) are qualitatively very similar to the experimentally measured temperature-dependent magnetization data in metallic $Ga_{1-x}Mn_xAs$ systems. In particular, recent annealing experiments, where annealing leads to better metallicity (e.g., higher conductivity) by virtue of increasing the hole density, show qualitative trends strikingly similar to the results of Fig. 4(a).

Next we include the direct antiferromagnetic coupling (4) between the local moments in our consideration. With $J^{AF} \neq 0$, the critical temperature is given by Eq. (20). The calculated impurity magnetization in the presence of the antiferromagnetic coupling is shown in Fig. 5. Comparing with the nondegenerate-hole model, we find that the degenerate-hole case is more quantitatively sensitive to the antiferromagnetic coupling although the qualitative effect of a finite $J^{AF}$ in both the metallic and the insulating DMS materials is basically the same, namely, suppression of the transition temperature and the magnetization.

Similar to the results shown for the insulating systems, we present in Fig. 5 calculated impurity magnetization for two values of the ratio $n_c/n_i=0.5$ [Fig. 5(a)] and 0.1 [Fig. 5(b)].

In Fig. 6, the calculated external magnetic field and temperature dependence of the dopant magnetization is shown for fixed parameter values $J,S,s$, and for various values of density ratio $n_c/n_i$. In the main figure, we show $M(T,B)$ as

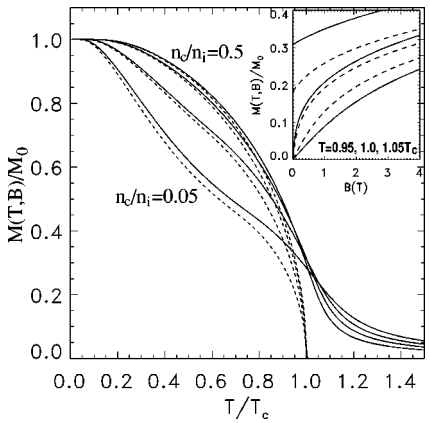


FIG. 6. External magnetic field and temperature dependence of dopant magnetization from the degenerate-hole model for various values of the density ratio ($n_c/n_i=0.5$, 0.2, 0.1, and 0.05, from the top). Solid (dashed) lines indicate the results for a fixed external magnetic field $B=2.6T$ ($0T$). The parameters in Fig. 4 are used. In the inset the magnetization curves as a function of magnetic field are given for fixed temperatures ($T=0.95$, 1.0, and $1.05T_c^{(d)}$, from the top). Solid (dashed) lines represent the results for $n_c/n_i=0.5$ ($n_c/n_i=0.05$).

a function of temperature for a magnetic-field value, $B=2.6T$ (solid lines), and in the inset, we show $M(T,B)$ as a function of the external field for fixed temperatures. Our calculated $M(T,B)$ behavior is roughly qualitatively similar to experimental observations in $Ga_{1-x}Mn_xAs$ systems in the metallic regime.

The magnetic susceptibility of the system is essentially that of impurities, similarly to Sec. II B 1, Eq. (16), and above the critical temperature is given by

$$\chi(T)=\frac{\chi_0+\dfrac{T_{c0}^{(d)}}{TJa_0^3}g_i g_c \mu_B^2}{1-\dfrac{T_c^{(d)}}{T}}, \tag{22}$$

where $\chi_0=n_i(g_i\mu_B)^2S(S+1)/3T$ is the paramagnetic susceptibility of bare impurities.

The Weiss molecular mean-field theory results (for localized carriers in Sec. II B 1 and for delocalized carriers in Sec. II B 2), presented above for DMS magnetization, qualitatively agree very well with the existing experimental data. In particular, the basic trend of our results shown in Figs. 1–6, that the spontaneous magnetization is strongly suppressed (perhaps even into a very unusual outwardly concave shape) at low carrier densities and for more insulating systems whereas at higher carrier densities and for more metallic systems, the magnetization has the usual convex textbook shape, is in excellent agreement with experiment. Our degenerate-carrier mean-field results [see Fig. 3(a)] also reproduce the almost linear magnetization curves seen in $Ga_{1-x}Mn_xAs$ for intermediate carrier densities. But obviously, one needs to go beyond the Weiss mean-field theory for a deeper (and more quantitative) understanding of DMS magnetization, if for no other reason than to validate (or to ascertain the regime of validity of) the simple static mean-field theory. At low carrier density, the mean-field theory should work better since on the average there are many Mn local moments between any two holes, but typically the number of Mn atoms per hole is around 3–4 so the quantitative applicability of MFT is questionable. Note that the hole-hole interaction neglected in our calculations may be included in a crude approximate fashion by incorporating a Stoner enhancement of the carrier susceptibility, though in general the strength of this enhancement is unknown.

In the next two sections, we go beyond the Weiss static mean-field theory and develop two more sophisticated approximation schemes to theoretically study DMS magnetization. These are DMFT (Sec. II C) and the percolation theory (Sec. II D).

### C. The Dynamical Mean-Field Theory

In this section, we use a recently developed nonperturbative method, the "dynamical mean-field theory" (DMFT),[38] to calculate magnetization for the minimal model [Eq. (2)] of dilute magnetic semiconductors. The DMFT has been recently applied to the DMS system to calculate the magnetic transition temperature and the optical conductivity.[22] DMFT is essentially a lattice quantum version of the Weiss mean-field theory, where the appropriate density of states (including impurity band formation) along with temporal fluctuations are incorporated within an effective local-field theory.

We model the $Ga_{1-x}Mn_xAs$ system as a lattice of sites, which are randomly nonmagnetic (with probability $1-x$) or magnetic (with probability $x$), where $x$ now indicates the relative concentration (i.e., per Ga site) of active Mn local moments in $Ga_{1-x}Mn_xAs$. The DMFT approximation amounts to assuming that the self-energy is local or momentum independent, $\Sigma(\mathbf{p},i\omega_n)\rightarrow\Sigma(i\omega_n)$, and then all of the relevant physics may be determined from the local (momentum-integrated) Green function defined by

$$G_{\rm loc}(i\omega_n)=a_0^3\int\frac{d^3p}{(2\pi)^3}\frac{1}{i\omega_n+\mu+h\sigma-\epsilon(p)-\Sigma_\sigma(i\omega_n)}, \tag{23}$$

where we have normalized the momentum integral to the volume of the unit cell $a_0^3$, and $\mu$ is the chemical potential and $h$ the external magnetic field. $G_{\rm loc}$ is, in general, a matrix in spin and band indices and depends on whether one is considering a magnetic ($a$) or nonmagnetic ($b$) site. Since $G_{\rm loc}$ is a local function, it is the solution of a local problem specified by a mean-field function $g_0$, which is related to the partition function $Z_{\rm loc}=\int d\mathbf{S}\exp(-S_{\rm loc})$ with action

$$S_{\rm loc}=\sum_{\alpha\beta}g^a_{0\alpha\beta}(\tau-\tau')c^\dagger_\alpha(\tau)c_\beta(\tau') + J\sum_{\alpha\beta}(\mathbf{S}\cdot\boldsymbol{\sigma}_{\alpha\beta})c^\dagger_\alpha(\tau)c_\beta(\tau'), \tag{24}$$

on the $a$ (magnetic) site and

$$S_{\rm loc}=\sum_{\alpha\beta}g^b_{0\alpha\beta}(\tau-\tau')c^\dagger_\alpha(\tau)c_\beta(\tau'), \tag{25}$$

on the (nonmagnetic) $b$ site. Here $c^\dagger_\alpha(\tau)$ ($c^\dagger_\alpha(\tau)$) is the destruction (creation) operator of a fermion in the spin state $\alpha$ and at time $\tau$. $g_0(\tau-\tau')$ plays the role of the Weiss mean field (bare Green function for the local effective action $S_{\rm loc}$) and is a function of time. Its physical content is that of an mean amplitude for a fermion to be created at time $\tau$ and being destroyed at time $\tau'$. The local Green function is calculated exactly as

$$G_{\rm loc}(i\omega_n)=\langle(g_0^{-1}+J\mathbf{S}\cdot\boldsymbol{\sigma}_{\alpha\beta})^{-1}\rangle, \tag{26}$$

where the thermal average $\langle\cdots\rangle$ is taken with respect to the orientation of the local spin $\mathbf{S}$. The $a$-site mean-field function $g_0^a$ can be written as $g^a_{0\alpha\beta}=a_0+a_1\mathbf{m}\cdot\boldsymbol{\sigma}_{\alpha\beta}$, with $\mathbf{m}$ the magnetization direction and $a_1$ vanishing in the paramagnetic state ($T>T_c$). Since the spin axis is chosen parallel to $\mathbf{m}$, $g_0^a$ becomes a diagonal matrix with components parallel ($g^a_{0\uparrow}=a_0+a_1$) and antiparallel ($g^a_{0\downarrow}=a_0-a_1$) to $\mathbf{m}$. It is specified by the condition that the local Green function computed from $Z_{\rm loc}$, namely, $\delta\ln Z_{\rm loc}/\delta g_0^a=(g_0^a-\Sigma)^{-1}$ is identical to the local Green function computed by performing the momentum integral using the same self-energy.

The form of the dispersion given in full Hamiltonian, Eq. (2), applies only near the band edges. It is necessary for the method to impose a momentum cutoff, arising physically from the carrier bandwidth. We impose the cutoff by assuming a semicircular density of states $D(\epsilon)=a_0^3\int d^3p/[(2\pi)^3]\delta(\varepsilon-\varepsilon_{pa})=\sqrt{4t^2-\epsilon^2}/2\pi t$, with $t=(2\pi)^{2/3}/ma_0^2$. The parameter $t$ is chosen to correctly reproduce the band edge density of states. Other choices of upper cutoff would lead to numerically similar results. This choice of cutoff corresponds to a Bethe lattice in infinite dimensions. Other (perhaps more realistic) choices for the density of states would give magnetization results qualitatively similar to our results since the band edge density of states has the correct physical behavior in our model. For this $N(\epsilon)$, the self-consistent equation for $g_0$ obeys the equation

$$\mathbf{g}_0^a(\omega)=\mathbf{g}_0^b(\omega)=\omega+\mu-xt^2\langle(\mathbf{g}_0^a(\omega)+J\mathbf{S}\cdot\sigma_{\alpha\beta})^{-1}\rangle - (1-x)t^2\langle\mathbf{g}_0^b(\omega)^{-1}\rangle, \tag{27}$$

where the angular brackets denote averages performed in the ensemble, defined by the appropriate $Z_{\rm loc}$.

Within this approximation, the normalized magnetization $M(T)$ of the local moments is given by

$$M(T)=\int (d\mathbf{S})\cdot\hat{\mathbf{S}}\frac{\exp(-S_{\rm loc})}{Z_{\rm loc}}. \tag{28}$$

As the temperature is increased, the spins disorder and eventually the magnetic transition temperature is reached. Above this temperature, $g_0$ is spin independent. By linearizing the equation in the magnetic part of $g_0$ with respect to $a_1$, we may obtain the ferromagnetic transition temperature $T_c$. The details on the calculation of $T_c$ are given in Ref. 22. The critical temperature $T_c$ and magnetization of the local moment depend crucially on $J/t$, $x$, and carrier density $n_c$. Note that in the DMFT calculation, it is more convenient to express our results in terms of $n$, the relative concentration of active local moments rather than $n_i$, the absolute impurity density.

Before we show our calculated magnetization, we describe the density of state (DOS) of dynamical mean-field calculations applying to simple semicircle models. In Fig. 7, we show the DMFT density of states for majority spin near the band edge corresponding to the disordered spin state $T>T_c$, and the inset shows the $T=0$ ferromagnetic state. The evolution of the energy ($\omega$) dependent DOS is shown as the carrier-spin coupling $J$ is increased from zero; note that the method works equally well in the ordered $T=0$ state and the disordered spin $T>T_c$ case, and predicts the formation of a spin-polarized impurity band for $J>t$. For small $J$, we see the expected band shift proportional to $xJ$. For $J>J_c$, an impurity band centered at $\sim -J$ and containing $x$ states, is seen to split off from the main band, where the critical coupling $J_c\sim t$. In the DMFT calculations, we parametrized the exchange coupling $J$ in terms of the bandwidth parameter $t$, subsuming the unit cell volume $a_0^3$ implicitly.

In Fig. 8, we show the normalized magnetization of the local moments as a function of temperature for different values of $J=1.0,1.5,2.0t$ and $x=0.05$, and for various hole densities, $n_c/n_i$. For the small coupling constant $J=t$, the impurity band is not formed, but for $J=1.5,2.0t$, we have a spin-polarized impurity band. For relatively high density ($n_c/n_i=0.4$, or $n=0.02$), the calculated magnetization looks similar to the Weiss mean-field results. But for low density ($n_c/n_i=0.04$), we have a linear $M(T)$ in the intermediate temperature range. Near the critical temperature $T_c$, the critical behavior of the magnetization for all density is given by $M(T)\propto(T_c-T)^{1/2}$. For different exchange couplings, we have similar results (i.e., linear behavior at low densities and intermediate temperature ranges).

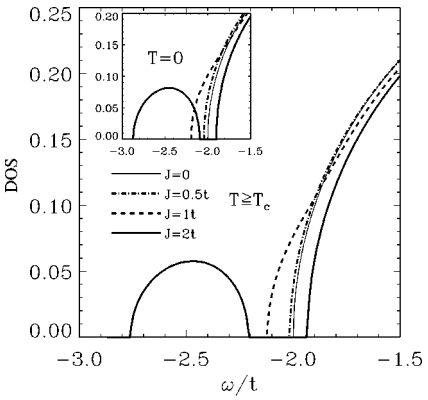


FIG. 7. The calculated density of states for dynamical mean-field calculations applied to the semicircular model. Shown is the evolution of majority spin DOS for various carrier-spin coupling $J$ in the disordered spin $T>T_c$ state. Inset shows the DOS for the ordered ferromagnetic state at $T=0$. For the large coupling constant $J>J_c$, we find a well separated impurity band below the main band.

In discussing our DMFT magnetization calculations, we note that the DMFT results shown in Fig. 8 are qualitatively roughly similar to the delocalized static (degenerate) mean-field-theory results we obtained in Sec. II B 2. For example, the results of Fig. 8 approximately resemble those shown in Fig. 4(a), except that the DMFT results of Fig. 8 are in much better agreement with the magnetization measurements in metallic $Ga_{1-x}Mn_xAs$ systems in the sense that the linear behavior of $M(T)$ for lower $T$ (with almost a kink just below $T_c$ as can be seen in Fig. 8) is much more pronounced (as in the experimental data) than our delocalized mean-field-theory results shown in Fig. 4(a). This is both gratifying and expected because DMFT is a substantial improvement on the Weiss mean-field theory (MFT) as it incorporates the physics of spin-split impurity bands through the appropriate quantum self-energy corrections not included in the simple MFT of Sec. II B. In fact, for very low carrier densities, we obtain outwardly concave $M(T)$ in our DMFT calculations (as we expect to do in the strongly nondegenerate limit), but the computational convergence in our DMFT numerical calculations is rather poor in this regime of unrealistically low ($n_c/n_i\lesssim 0.01$) carrier densities, and, therefore, we refrain from showing these results. One can, however, detect very slight concavity in the lowest carrier density ($n_c/n_i=0.04$) $M(T)$ results shown in Fig. 8. We point out that the critical magnetic properties in DMFT are the same as in the static

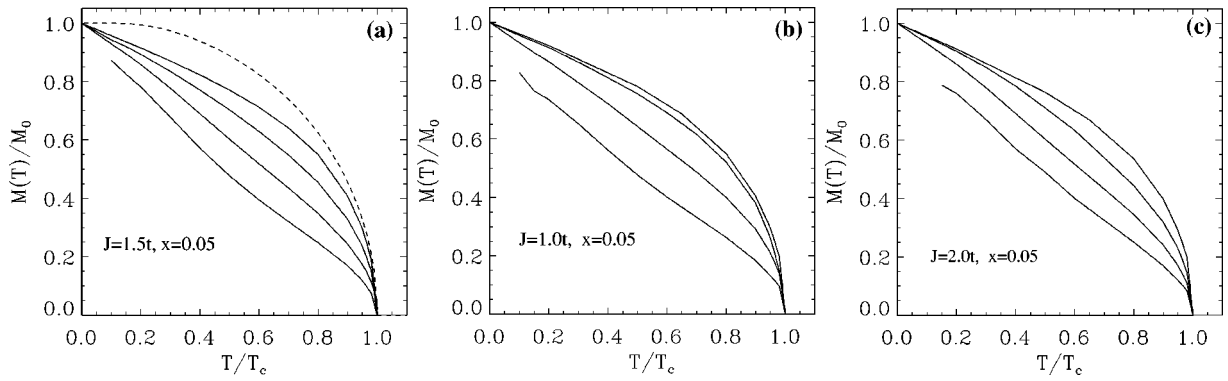


FIG. 8. The normalized DMFT impurity magnetization as a function of temperature for (a) $J=1.5t$, (b) $J=1.0t$, and (c) $J=2.0t$; for $x=0.05$ and for $n_c/n_i=0.4$, 0.2, 0.1, and 0.04 (from the top). The dashed line in (a) represents the magnetization calculated for the simple Weiss mean-field theory for the local-moment spin $S=5/2$.

MFT, and therefore, all the DMFT critical exponents are equal to those in the Weiss MFT.

In particular, it should be possible to obtain the $M(T)$ behavior for the localized carrier case (cf. Sec. II B 1) also from DMFT by incorporating impurity band localization in the DMFT formalism. Our current theory does not include localization, and the impurity band (or valence-band) carriers in our DMFT calculations are all delocalized metallic carriers. First-principles band theory calculations indicate that the actual exchange coupling in $Ga_{1-x}Mn_xAs$ may be close to critical $J_c$, and as such impurity band physics may be quite important for understanding DMS magnetization. To incorporate physics of localization, one needs to include disorder effects (invariably present in real DMS systems) in the model. All our MFT calculations (both DMFT in Sec. II C and the static MFT of Sec. II B) are done in the virtual crystal approximation, where effective field is averaged appropriately leaving out random disorder effects explicitly. In the following section, we explicitly incorporate disorder in the theory by developing a percolation theory approach to DMS magnetization for the strongly localized insulating systems.

The calculated magnetization as a function of temperature is shown in Fig. 9 for various external magnetic-field values. The inset shows the magnetization as a function of external field at $T=T_c$. Our calculated $M(T,B)$ behavior is roughly qualitatively similar to the mean-field results in Sec. II B 2. At the critical temperature $T_c$, $M(T_c,B)$ shows a mean-field behavior, $M(T_c,B)\propto B^{1/3}$. The DMFT results shown in Fig. 9 are qualitatively similar to DMS experimental results.

### D. Magnetization in the percolation formalism

Our recently developed percolation theory[9] applies strictly in the regime of strongly localized holes, where the dynamical mean-field theory for delocalized carriers described in Sec. II C has little validity. These two theories, mean-field theory and percolation theory, are, therefore, complementary. Interestingly, however, the perturbation theory and the dynamical mean-field theory are not mutually exclusive in spite of their regimes of validity being different, and in particular, a significant aspect of our percolation approach is its ability to reproduce qualitatively the mean-field-theory results of the preceding section both for $T_c$ and $M(T)$.

The percolation theory assumes the same carrier-mediated ferromagnetism model of Sec. II B, but now the carriers are pinned down with the localization radius $a_B$. The localized carriers are therefore taken to be in the impurity band and disorder, completely neglected in the mean-field theory of Secs. II B and II C, now plays a key role in the carrier localization. The mean-field theory and the perturbation theory are therefore, complementary in the sense that one (the mean-field theory) completely neglects disorder, and the other (the percolation theory) includes disorder at a very fundamental level, i.e., by starting from the picture of localized carriers in a strongly disordered system. The magnetic impurities in this case are assumed to be completely randomly distributed in the host semiconductor lattice in contrast to the mean-field case, where the carrier states are free and the disorder is neglected.

As we have demonstrated in Ref. 9, the problem of ferromagnetic transition in a system of bound magnetic polarons can be rigorously reduced to the problem of overlapping spheres studied in the percolation theory.[23] The latter problem studies spheres of the same radius $r$ randomly placed in

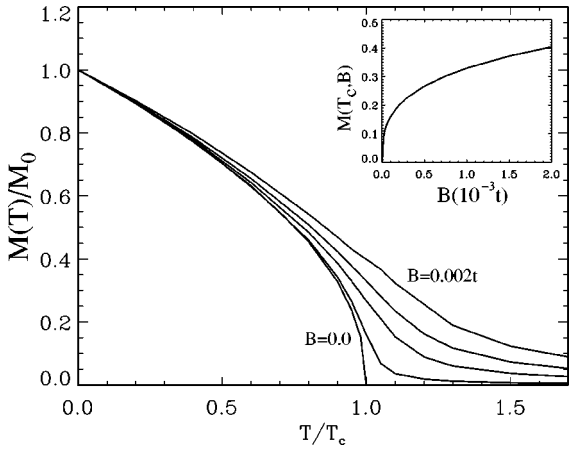


FIG. 9. The external magnetic-field effects on the magnetization as a function of temperature for fixed parameter values $J=1.5t$, $x=0.05$, and $n_c/n_i=0.2$. The curves correspond to $B=0.002$, 0.001, 0.0005, 0.0001, and 0.0t (from the top). Inset shows the magnetization as a function of external field at $T=T_c$.

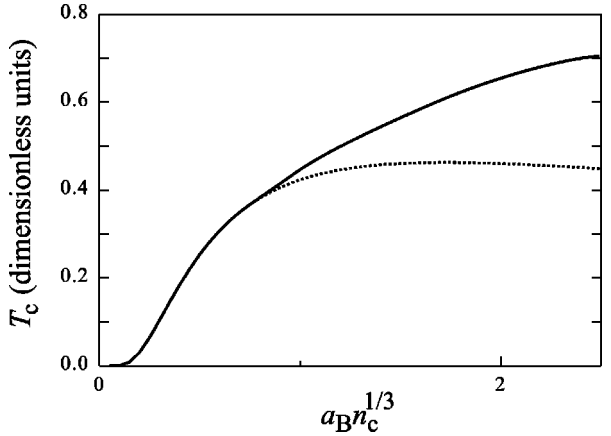


FIG. 10. Curie temperature $T_c$ as a function of the dimensionless parameter $a_B^3 n_c$. At $a_B^3 n_c \lesssim 1$, $T_c$ is given by Eq. (30). At $a_B^3 n_c \gtrsim 1$, Eq. (30) (being beyond limits of its applicability) predicts decline of $T_c$ (dotted line); in reality, $T_c$ grows monotonically with $a_B^3 n_c$ (solid line), though its exact behavior is unknown.

space (three-dimensional in our case) with some concentration $n$. Overlapping spheres form ''clusters''; as the sphere radius $r$ becomes larger, more and more spheres join into clusters, the clusters coalesce, and finally, at some critical value of the sphere radius, an infinite cluster spanning the whole sample appears. This problem has only one dimensionless parameter $r^3 n$ and, therefore, can be easily studied by means of Monte-Carlo simulations.

Each sphere of the overlapping spheres problem corresponds to a bound magnetic polaron, which is a complex formed by one localized hole and many magnetic impurities with their spins polarized by the exchange interaction with the hole spin. The concentration $n$ of spheres is therefore, equal to the concentration $n_c$ of localized holes. The expression for the effective polaron radius is not trivial and has been found in our earlier work.[9] The resulting formal relation between the physical parameters of the system under consideration and the only parameter of the overlapping spheres problem reads:[9]

$$r^3 n = \left[ 0.86 + (a_B^3 n_c)^{1/3} \ln \frac{T_c}{T} \right]^3. \tag{29}$$

Here $0.64 \approx 0.86^3$ is the critical value of the parameter $r^3 n$, at which the infinite cluster appears, and $T_c$ is the Curie temperature of the ferromagnetic system under consideration, derived in Ref. 9,

$$T_c \sim sSJ \left( \frac{a_0}{a_B} \right)^3 (a_B^3 n_c)^{1/3} \sqrt{\frac{n_i}{n_c}} \exp\left( - \frac{0.86}{(a_B^3 n_c)^{1/3}} \right). \tag{30}$$

The limit of applicability of Eq. (30) is determined by the condition $a_B^3 n_c \ll 1$. The dependence of the Curie temperature on the hole concentration in a wider domain of values of parameter $a_B^3 n_c$ is shown schematically in Fig. 10.

Since the magnetic characteristics of the sample are mostly due to magnetic impurities rather than holes, the quantity of interest is the number of magnetic impurities in a cluster, which is proportional to the cluster volume. The magnetic properties of the system can be expressed in terms of the following quantities, which can be easily found: (i) concentration $\mathcal{P}(vn; r^3 n) dv$ of clusters with volume between $v$ and $v + dv$, (ii) the fraction of volume $P_\infty(r^3 n)$ taken by the infinite cluster, and (iii) the fraction $P_0(r^3 n)$ that does not belong to any sphere or cluster of spheres. Clearly, these quantities obey the relation

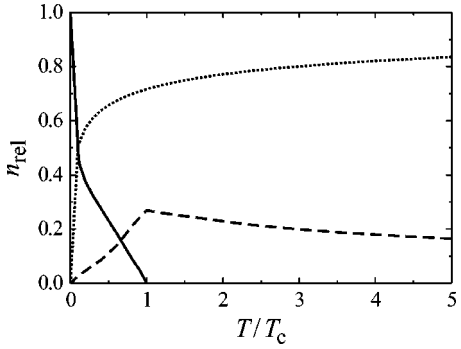


FIG. 11. Fractions of volume taken by the infinite cluster (solid line) and finite clusters (dashed line) and the fraction of volume that do not belong to any cluster or sphere (dotted line) for $a_B^3 n_c = 10^{-3}$ (Monte-Carlo simulation).

$$P_\infty(rn^{1/3}) + \int_0^\infty \mathcal{P}(vn; rn^{1/3}) v\, dv + P_0(rn^{1/3}) \equiv 1.$$

Figure 11 shows the behavior of the three terms of the above equation as a function of temperature $T$, with $r^3 n$ related to $T/T_c$ by Eq. (29) and $a_B^3 n_c = 10^{-3}$. Having found these quantities, one can easily find the magnetic properties of the system.

The spins of nonconnected clusters are not correlated and average out when we calculate the spontaneous magnetization of the whole sample. The only nonvanishing contribution comes from the infinite cluster. The total magnetic moment of the sample per unit volume is, therefore,

$$M = n_i S P_\infty \left( \frac{T}{T_c}, a_B^3 n_c \right). \tag{31}$$

Here and in the following equations, we write the characteristics $P_\infty$, $P_0$, and $\mathcal{P}(vn)$ of the overlapping sphere problem as functions of the physical parameters $T/T_c$ and $a_B^3 n_c$ instead of $r^3 n$. The relation between these parameters is given by Eq. (29). The temperature dependence of the spontaneous magnetization given by Eq. (31) is plotted in Fig. 12 for two experimentally variable values of $a_B^3 n_c$. As already mentioned before, such strongly concave $M(T)$ behavior is often observed in insulating DMS systems, see, for example, Refs. 4,6, and 39.

The magnetic susceptibility of a sample has contributions coming from polaron clusters and free spins. Using the classical expression for the susceptibility of a free magnetic moment $m_0$

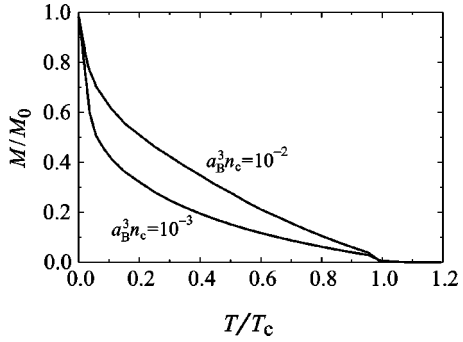


FIG. 12. Spontaneous magnetization as a function of temperature.

$$\chi_{m_0}=\frac{m_0^2}{3T},$$

and the fact that the total spin of a cluster with volume $v$ equals $vn_{\mathrm{i}}$, we arrive at

$$\chi=\frac{1}{3T}gS^2\left[\int_0^\infty \mathcal{P}\left(vn_{\mathrm{c}};\frac{T}{T_c},a_B^3n_{\mathrm{c}}\right)(vn_{\mathrm{i}})^2dv + n_{\mathrm{i}}P_0\left(\frac{T}{T_c},a_B^3n_{\mathrm{c}}\right)\right]. \tag{32}$$

The first term in brackets diverges as $(T-T_c)^\gamma$ with $\gamma \approx 1.7$ at $T\to T_c$. The second term in brackets does not have any singularity at $T\to T_c$. For the temperature dependence of the susceptibility given by Eq. (32), see Fig. 13.

Using the classical magnetization relation

$$M_S(T)=S\mathcal{L}\left(\frac{g_{\mathrm{i}}\mu_B SB}{T}\right), \tag{33}$$

where $\mathcal{L}(x)\equiv\mathcal{B}_\infty(x)=\mathrm{cotan}x-1/x$ is the Langevin function, we obtain the following expression for the magnetic moment per unit volume in finite magnetic field:

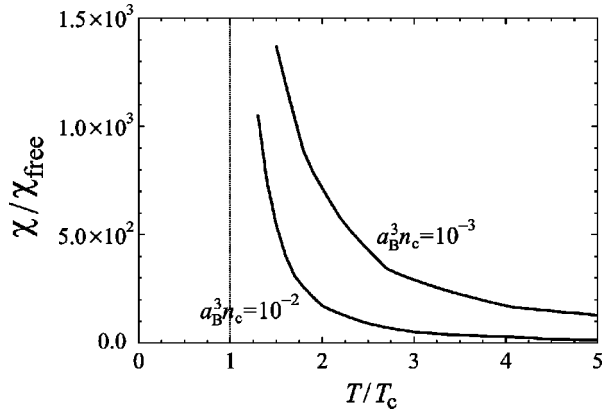


FIG. 13. Temperature dependence of the magnetic susceptibility for $n_{\mathrm{c}}/n_{\mathrm{i}}=0.02$.

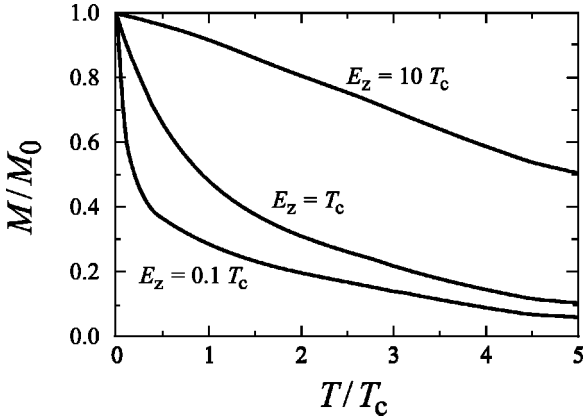


FIG. 14. Temperature dependence of magnetization in finite magnetic field with $E_Z=g_{\mathrm{i}}\mu_B SB$.

$$M(B)=n_{\mathrm{i}}SP_\infty\left(\frac{T}{T_c},a_B^3n_{\mathrm{c}}\right) + \int_0^\infty \mathcal{P}\left(vn_{\mathrm{c}};\frac{T}{T_c},a_B^3n_{\mathrm{c}}\right)vn_{\mathrm{i}}\mathcal{L}\left(\frac{g_{\mathrm{i}}\mu_B vn_{\mathrm{i}}SB}{T}\right)dv + n_{\mathrm{i}}SP_0\left(\frac{T}{T_c},a_B^3n_{\mathrm{c}}\right)\mathcal{L}\left(\frac{g_{\mathrm{i}}\mu_B SB}{T}\right). \tag{34}$$

Figures 14 and 15 illustrate the dependence of the magnetization on the temperature and magnetic field, respectively. Since the spins of polarons and their clusters are much large than those of three impurities, the magnetization curve of Fig. 15 has two characteristic scales. First, polarons and their clusters are polarized (inset of Fig. 15), then the free spins are polarized at much larger fields.

We mention that our percolation-theory critical exponents are $\gamma\approx 1.7$ and $\beta\approx 0.4$ for the susceptibility (Fig. 13) and magnetization (Fig. 12), as compared with the mean-field results of $\gamma=1$ and $\beta=0.5$ and the best existing numerical estimates of $\gamma\approx 1.39$ and $\beta\approx 0.37$ for the three-dimensional Heisenberg model.[40]

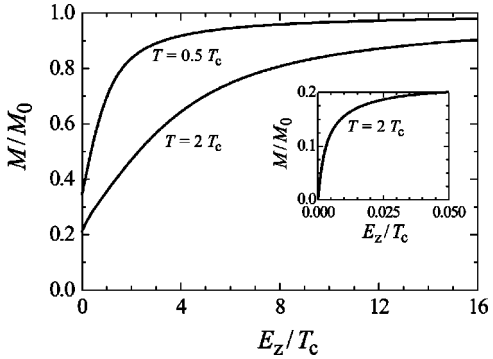


FIG. 15. Magnetic-field dependence of the sample magnetization at given temperature with $E_Z=g_{\mathrm{i}}\mu_B SB$.

## III. CONCLUSION

The temperature-dependent magnetization results presented in this work for different but interrelated theoretical models are qualitatively consistent with one another. In particular, the two theories for metallic DMS systems with itinerant carriers, namely, the degenerate-carrier Weiss static mean-field theory (see Sec. II B 2) and the dynamical mean-field theory (see Sec. II C), both give onwardly convex $M(T)$ carriers, similar (but not identical) to that in the textbook molecular mean-field result, with the convexity being enhanced (suppressed) with increasing (decreasing) delocalized carrier density. In typical situations involving itinerant carriers in metallic DMS systems, we find temperature-dependent magnetization curves that are almost linear at lower temperatures, in excellent agreement with experimental observations in metallic $Ga_{1-x}Mn_xAs$ systems. Such apparent ''non-mean-field-like'' magnetization behavior, found here both in our delocalized-carrier static and dynamic mean-field theories, arises from a combination of following reasons: (1) the double Brillouin function [i.e., $\mathcal{B}(\mathcal{B}(x))$] form of the coupled field magnetization [see Eq. (9)]; (2) the low values of $n_c/n_i$, leading to the Mn moments feeling on the average a much reduced number of free carriers. As the carrier density is increased, for example, by suitable annealing in recent experimental studies, such linear magnetization curves evolve toward the more conventional outwardly convex magnetization, as can be seen in our results and in recent annealing experiments.[15–19] In the case of localized carriers appropriate for insulating DMS systems [many of which are also found to be ferromagnetic with well-defined Curie temperatures, e.g., $Ga_{1-x}Mn_xAs$ for $x<0.03$, $In_{1-x}Mn_xAs$,[4] and $Ge_{1-x}Mn_x$ (Ref. 6)], our two complementary theories, namely the nondegenerate-carrier static mean-field theory (Sec. II B 1) and the percolation theory (Sec. II D), give qualitatively similar magnetization behavior. In particular, at low carrier densities the $M(T)$ curves in strongly insulating DMS systems exhibit strikingly non-mean-field-like outwardly concave magnetization behavior, as often observed in the insulating DMS systems. Again, this unusual concave magnetization behavior arises from a combination of the strongly localized nature of the carrier system and the low values of the carrier density (i.e., $n_c/n_i \ll 1$) in DMS materials. We emphasize, however, a very important feature of theoretical results presented in this work: the convex magnetization behavior in the strongly metallic case and the concave behavior in the insulating case are *not* a sharp dichotomy in DMS properties—these are really the two extremes of a continuum of possible magnetization behavior in DMS materials, as can be inferred from the results of Sec. II B. The typical DMS magnetization behavior should lie somewhere in between these two extremes of highly concave (low carrier density and strongly localized insulating DMS) and highly convex (high carrier density and strongly delocalized metallic DMS) magnetization, leading to the generic experimental observation of almost linear $M(T)$ behavior in ferromagnetic $Ga_{1-x}Mn_xAs$.

Another often-mentioned peculiar aspect of DMS magnetization, namely, the low value of the saturation magnetization (compared with the number of Mn ions in the sample as given by the value of $x$ in $Ga_{1-x}Mn_xAs$), is also apparent in our theoretical results presented in this work. In particular, the presence of direct antiferromagnetic coupling between the Mn moments may drastically suppress the saturation magnetization, as can be seen in the results presented in Figs. 2 and 5 of this paper. This absence of complete magnetization saturation in our mean-field results is akin to having effective ferrimagnetism in the system. In addition, the calculated magnetization is may be much lower than the saturation value except at very low temperatures, see Fig. 12, which could also explain the lack of magnetization saturation. It is likely that in the real DMS materials an appreciable fraction of the Mn moments are magnetically inactive because they do not sit in cation substitutional sites, but rather at defect sites such as interstitials and are antiferromagnetically coupled to other Mn moments. Such magnetically inactive Mn atoms could be one of the reasons for the low values of saturation magnetization in $Ga_{1-x}Mn_xAs$. We also note that our percolation theory provides another possible explanation for the observed low values of saturation magnetization in low carrier density insulating DMS materials. Since the infinite cluster of percolating bound magnetic polarons triggering the long-range ferromagnetic ordering necessarily leaves out a large number of Mn moments (which are not parts of the infinite cluster except at $T \to 0$), one naturally expects a very low saturation magnetization except perhaps at $T \ll T_c$.

A recent series of potentially important annealing experiments in metallic $Ga_{1-x}Mn_xAs$ samples by several different groups may eventually shed considerable light on our understanding of the mechanisms underlying DMS ferromagnetism. These experiments, while differing somewhat on the details, all find that suitable low temperature optimal annealing may enhance the magnetic properties of $Ga_{1-x}Mn_xAs$ by increasing $T_c$ and more importantly for our purpose, by enhancing $M(T)$ to more convex almost standard mean-field-like behavior. This enhancement of magnetization seems to correlate well with improvement in the metallicity of the annealed sample (e.g., higher conductivity) and with an increase in the hole density. Annealing may also be enhancing the magnetic properties by annealing away some of the Mn interstitials. Our theoretical results are in excellent agreement with these annealing experiments, since increasing $n_c/n_i$ does lead to enhanced (and more convex) magnetization in our theory. In this context, it will be very helpful to have more detailed information on the $M(T)$ behavior in strongly localized insulating samples both for $Ga_{1-x}Mn_xAs$ with $x<0.03$ and for other insulating DMS materials (e.g., $Ge_{1-x}Mn_x$).

Our final comment addresses the role of disorder (essentially neglected in our work, except for the percolation theory part, as we treat it in the virtual crystal approximation, i.e., we assume that holes and local moments only feel the average effective field), which is invariably strong (and not yet well understood) in DMS materials. In particular, even the metallic DMS systems are in effect very poor metals with mean-free paths which are at or below the Ioffe-Regel limit (with low-temperature mobilities of the order of a few

$cm^2/V\,s$ only), indicating the presence of very strong disorder.[41] In the presence of such strong disorder, various spin-glass ground states may compete with ferromagnetic ground states. We believe that it is important to look for signatures of spin-glass physics in low-temperature DMS magnetic properties. It may very well turn out that spin-glass phases dominate the regime of parameter space (e.g., $x<1\%$ or $x>10\%$ in $Ga_{1-x}Mn_xAs$), where a ferromagnetic ground state does not seem to stabilize in DMS materials.

## ACKNOWLEDGMENTS

This work was supported by US-ONR and DARPA.

[1] H. Ohno, Science **281**, 951 (1998); J. Magn. Magn. Mater. **200**, 110 (1999).

[2] R.N. Bhatt, M. Berciu, M. Kennett, and X. Wan, J. Supercond. **15**, 71 (2002); S. Sanvito, G. Theurich, and N.A. Hill, *ibid.* **15**, 85 (2002); T. Dietl, Semicond. Sci. Technol. **17**, 377 (2002); B. Lee, T. Jungwirth, and A.H. MacDonald, *ibid.* **17**, 393 (2002).

[3] H. Ohno, A. Shen, F. Matsukura, A. Oiwa, A. Endo, S. Katsumoto, and Y. Iye, Appl. Phys. Lett. **69**, 363 (1996).

[4] H. Ohno, H. Munekata, T. Penney, S. von Molnár, and L.L. Chang, Phys. Rev. Lett. **68**, 2664 (1992).

[5] N. Theodoropoulou, A.F. Hebard, M.E. Overberg, C.R. Abernathy, S.J. Pearton, S.N.G. Chu, and R.G. Wilson, Phys. Rev. Lett. **89**, 107203 (2002).

[6] Y.D. Park, A.T. Hanbicki, S.C. Irwin, C.S. Hellberg, J.M. Sullivan, J.E. Mattson, T.F. Ambrose, A. Wilson, G. Spanos, and B.T. Jonker, Science **295**, 651 (2002).

[7] X. Chen, M. Na, M. Cheon, S. Wang, H. Luo, B.D. McCombe, X. Liu, Y. Sasaki, T. Wojtowicz, J.K. Furdyna, S.J. Potashnik, and P. Schiffer, Appl. Phys. Lett. **81**, 511 (2002).

[8] M.W. Ashcroft and N.D. Mermin, *Solid State Physics* (Saunders College, Philadelphia, 1976); C. Kittel, *Introduction to Solid State Physics* (Wiley, New York, 1996).

[9] A. Kaminski and S. Das Sarma, Phys. Rev. Lett. **88**, 247202 (2002).

[10] M.P. Kennett, M. Berciu, and R.N. Bhatt, Phys. Rev. B **66**, 045207 (2002); M. Berciu and R.N. Bhatt, Phys. Rev. Lett. **87**, 107203 (2000).

[11] M.J. Calderón, G. Gómez-Santos, and L. Brey, Phys. Rev. B **66**, 075218 (2002).

[12] M. Mayr, G. Alvarez, and E. Dagotto, Phys. Rev. B **65**, 241202 (2002).

[13] T. Hayashi, Y. Hashimoto, S. Katsumoto, and Y. Iye, Appl. Phys. Lett. **78**, 1691 (2001); T. Hayashi, Y. Hashimoto, S. Yoshida, S. Katsumoto, and Y. Iye, Physica E (Amsterdam) **10**, 130 (2001).

[14] K.M. Yu, W. Walukiewicz, T. Wojtowicz, I. Kuryliszyn, X. Liu, Y. Sasaki, and J.K. Furdyna, Phys. Rev. B **65**, 201303 (2002)

[15] S.J. Potashnik, K.C. Ku, S.H. Chun, J.J. Berry, N. Samarth, and P. Schiffer, Appl. Phys. Lett. **79**, 1495 (2001); S.J. Potashnik, K.C. Ku, R. Mahendiran, S.H. Chun, R.F. Wang, N. Samarth, and P. Schiffer, cond-mat/0204250 (unpublished).

[16] K.W. Edmonds, K.Y. Wang, R.P. Campion, A.C. Neumann, N.R.S. Farley, B.L. Gallagher, and C.T. Foxon, cond-mat/0209554 (unpublished); cond-mat/0209123 (unpublished); cond-mat/0205517 (unpublished).

[17] I. Kuryliszyn, T. Wojtowicz, X. Liu, J.K. Furdyna, W. Dobrowolski, J.-M. Broto, M. Goiran, O. Portugall, H. Rakoto, and B. Raquet, cond-mat/0207354 (unpublished); cond-mat/0206371 (unpublished).

[18] R. Mathieu, B.S. Sørensen, J. Sadowski, J. Kanski, P. Svedlindh, and P.E. Lindelof, cond-mat/0208411 (unpublished).

[19] K.C. Ku, S.J. Potashnik, R.F. Wang, M.J. Seong, E. Johnston-Halperin, R.C. Meyers, S.H. Chun, A. Mascarenhas, A.C. Gossard, D.D. Awschalom, P. Schiffer, and N. Samarth, cond-mat/0210426 (unpublished).

[20] A. Van Esch, L. Van Bockstal, J. De Boeck, G. Verbanck, A.S. van Steenbergen, P.J. Wellmann, B. Grietens, R. Bogaerts, F. Herlach, and G. Borghs, Phys. Rev. B **56**, 13 103 (1997).

[21] T. Dietl, H. Ohno, and F. Matsukura, Phys. Rev. B **63**, 195205 (2001).

[22] A. Chattopadhyay, S. Das Sarma, and A.J. Millis, Phys. Rev. Lett. **87**, 227202 (2001); E.H. Hwang, A.J. Millis, and S. Das Sarma, Phys. Rev. B **65**, 233206 (2002).

[23] B.I. Shklovskii and A.L. Efros, *Electronic Properties of Doped Semiconductors* (Springer-Verlag, Berlin, 1984).

[24] B. Beschoten, P.A. Crowell, I. Malajovich, D.D. Awschalom, F. Matsukura, A. Shen, and H. Ohno, Phys. Rev. Lett. **83**, 3073 (1999).

[25] T. Hayashi, S. Katsumoto, Y. Hashimoto, A. Endo, M. Kawamura, M. Zalalutdinov, and Y. Iye, Physica B **284-288**, 1175 (2000).

[26] J. Okabayashi, A. Kimura, O. Rader, T. Mizokawa, A. Fujimori, T. Hayashi, and M. Tanaka, Physica E (Amsterdam) **10**, 192 (2001).

[27] E.J. Singley, R. Kawakami, D.D. Awschalom, and D.N. Basov, Phys. Rev. Lett. **89**, 097203 (2002).

[28] S. Sanvito, P. Ordejón, and N.A. Hill, Phys. Rev. B **63**, 165206 (2001); M. van Schilfgaarde and O.N. Mryasov, *ibid.* **63**, 233205 (2001); S.C. Erwin and A.G. Petukhov, Phys. Rev. Lett. **89**, 227201 (2002).

[29] J. Szczytko, W. Mac, A. Twardowski, F. Matsukura, and H. Ohno, Phys. Rev. B **59**, 12 935 (1999).

[30] A.K. Bhattacharjee, Phys. Rev. B **46**, 5266 (1992).

[31] T. Kasuya, in *Magnetism*, edited by G.T. Rado and H. Suhl (Academic Press, New York, 1966), Vol. III B, p. 215.

[32] C. Zener, Phys. Rev. **81**, 446 (1951); **82**, 403 (1951); **83**, 229 (1951).

[33] F. Fröhlich and F.R.N. Nabarro, Proc. R. Soc. London, Ser. A **175**, 382 (1940).

[34] M. Sigrist, K. Ueda, and H. Tsunetsugu, Phys. Rev. B **46**, 175 (1992); S. Doniach, Physica B **91**, 231 (1977); P. Nozières, Eur. Phys. J. B **6**, 447 (1998); A.N. Tahvildar-Zadeh, M. Jarrell, and J.K. Freericks, Phys. Rev. B **55**, R3332 (1997).

[35] A.A. Abrikosov and L.P. Gorkov, Zh. Eksp. Teor. Fiz. **43**, 2230 (1962) [Sov. Phys. JETP **16**, 1575 (1963)]. Rather ironically this

paper dealt with the Zener-RKKY model of impurity ferromagnetism in metallic systems, where the carrier density is much larger than the local-moment density (in contrast to DMS materials, where $n_i \gg n_c$)—it is now well known that RKKY interaction in disordered magnetic alloy systems (e.g., Cu-Mn) leads to spin-glass-type behavior rather than ferromagnetism; nevertheless the mean-field-theory expression for $T_c$ derived in this paper is precisely the same as our Eq. (20), which is used in much of the DMS literature in discussing the Curie temperature.

[36] T. Dietl, H. Ohno, F. Matsukura, and D. Ferrand, Science **287**, 1019 (2000).

[37] T. Jungwirth, W.A. Atkinson, B.H. Lee, and A.H. MacDonald, Phys. Rev. B **59**, 9818 (1999).

[38] A. Georges, G. Kotliar, W. Krauth, and M.J. Rozenberg, Rev. Mod. Phys. **68**, 13 (1996).

[39] G.H. McCabe, T. Fries, M.T. Liu, Y. Shapira, L.R. Ram-Mohan, R. Kershaw, A. Wold, C. Fau, M. Averous, and E.J. McNiff, Jr., Phys. Rev. B **56**, 6673 (1997).

[40] A. Pelissetto and E. Vicari, Phys. Rep. **368**, 549 (2002).

[41] C. Timm, F. Schäfer, and F. von Oppen, Phys. Rev. Lett. **89**, 137201 (2002).